Journal of Molecular Graphics and Modelling 41 (2013) 79–88

Contents lists available at SciVerse ScienceDirect

Journal of Molecular Graphics and Modelling

journal homepage: www.elsevier.com/locate/JMGM

Third-order nonlinear optical properties of molecules containing aromatic diimides: Effects of the aromatic core size and a redox-switchable modification

Yong-Qing Qiu [a,b,*], Zhuo Li [b], Na-Na Ma [b], Shi-Ling Sun [b], Meng-Ying Zhang [b], Peng-Jun Liu [a,**]

[a] College of Chemistry & Chemical Engineering, Hainan Normal University, Haikou 571158, People's Republic of China
[b] Institute of Functional Material Chemistry, Faculty of Chemistry, Northeast Normal University, Changchun 130024, People's Republic of China

ARTICLE INFO

Article history:
Accepted 29 January 2013
Available online 16 February 2013

Keywords:
Aromatic diimides
Aromatic core size
Redox
Radical anion
BLA value
NLO property

ABSTRACT

The third-order nonlinear optical (NLO) properties of aromatic diimide molecules have been studied for the first time using density functional theory (DFT) with a finite field (FF). This study shows that the size of the aromatic core can affect the static second hyperpolarizability (γ). Increasing the number of benzenes along the longitudinal axis can effectively improve the γ values because the degree of charge transfer along the longitudinal direction increases, whereas an increase in the number of benzenes along the perpendicular axis does not enhance the γ values. Furthermore, the NLO responses of the reduced form radical anions **1**$^{\bullet-}$, **5**$^{\bullet-}$ and **6**$^{\bullet-}$, which were obtained by a reversible redox process, are discussed. The results show that the γ values of the radical anions are changed by the redox process. For the reduced form radical anion **6**$^{\bullet-}$, the γ value is -1906.71×10^{-36} esu, and its absolute value is ~7.3 times larger than that of its neutral parent. An analysis of the BLA values demonstrates that the γ value is closely related to the conjugation of the aromatic core used in the redox process.

1. Introduction

Materials with excellent nonlinear optical (NLO) responses continue to be the focus of theoretical and experimental research [1–4]. Many organic molecules that exhibit highly efficient NLO properties have attracted considerable attention because of their potential applications in optical communication, optical data storage, photodynamic therapy, three-dimensional memory and photonic devices such as optical switches [5–7]. In particular, organic π-conjugated third-order NLO materials have been extensively studied because of their large second hyperpolarizabilities (γ) and their fast response times [8,9]. Moreover, much work on optimizing the third-order NLO responses has been performed, revealing that the amplitude and sign of the γ value can be adjusted by changing the bond length alternation, the strength of the donor/acceptor substituents, the charge and the size of the π-conjugation [10–13].

Aromatic diimides have been used widely in fundamental studies of photoinduced electron-transfer-containing models for photosynthesis [14,15], solar energy conversion [16], photorefractive materials [17], molecular electronics [18] and electrochromic devices [19]. Moreover, experimental research indicates that pyromellitic diimides, naphthalene diimides and perylene diimides are compact aromatic compounds with high stabilities and conjugated planes [20–22]. The research suggests that these aromatic diimide systems have potential applications in the NLO material field. The first hyperpolarizabilities (β) of donor–acceptor aromatic systems, which containing anthracene and naphthalene as electron donors and naphthadiimide and pyromellitimide as electron acceptors, were studied by changing the efficiency of electronic communication between donor and acceptor units of the molecular systems [23]. However, the third-order NLO responses of aromatic diimide systems have never been reported. We have therefore systematically studied the effect of the aromatic core size on the NLO properties of aromatic diimide systems. The third-order NLO responses are studied for two types of aromatic diimides: the five-membered aromatic diimide systems **1**–**4** and the six-membered aromatic diimide systems **5**–**7**, which contain nitrobenzene with an N-substituent (Scheme 1). To determine the effect of the aromatic core size on the NLO responses, systems **1–4** increased the number of benzene rings along the longitudinal or perpendicular axis with increasing system number. The six-membered aromatic diimide systems **5**–**7** were studied in a similar manner.

Reversible changes in the NLO properties of molecular materials are also interesting to study because these changes are useful for developing molecular switches [24,25], and NLO switches may have novel and interesting applications in optoelectronic technologies [26]. To achieve a pronounced switching of molecular NLO properties, the stability of two configurations relative to a switching

* Corresponding author at: Institute of Functional Material Chemistry, Faculty of Chemistry, Northeast Normal University, Changchun 130024, People's Republic of China. Tel.: +86 431 85099291; fax: +86 431 85098768.
** Corresponding author. Tel.: +86 431 85099291; fax: +86 431 85098768.
E-mail addresses: qiuyq466@nenu.edu.cn (Y.-Q. Qiu), liupj12@126.com (P.-J. Liu).

1093-3263/$ – see front matter © 2013 Elsevier Inc. All rights reserved.
http://dx.doi.org/10.1016/j.jmgm.2013.01.008

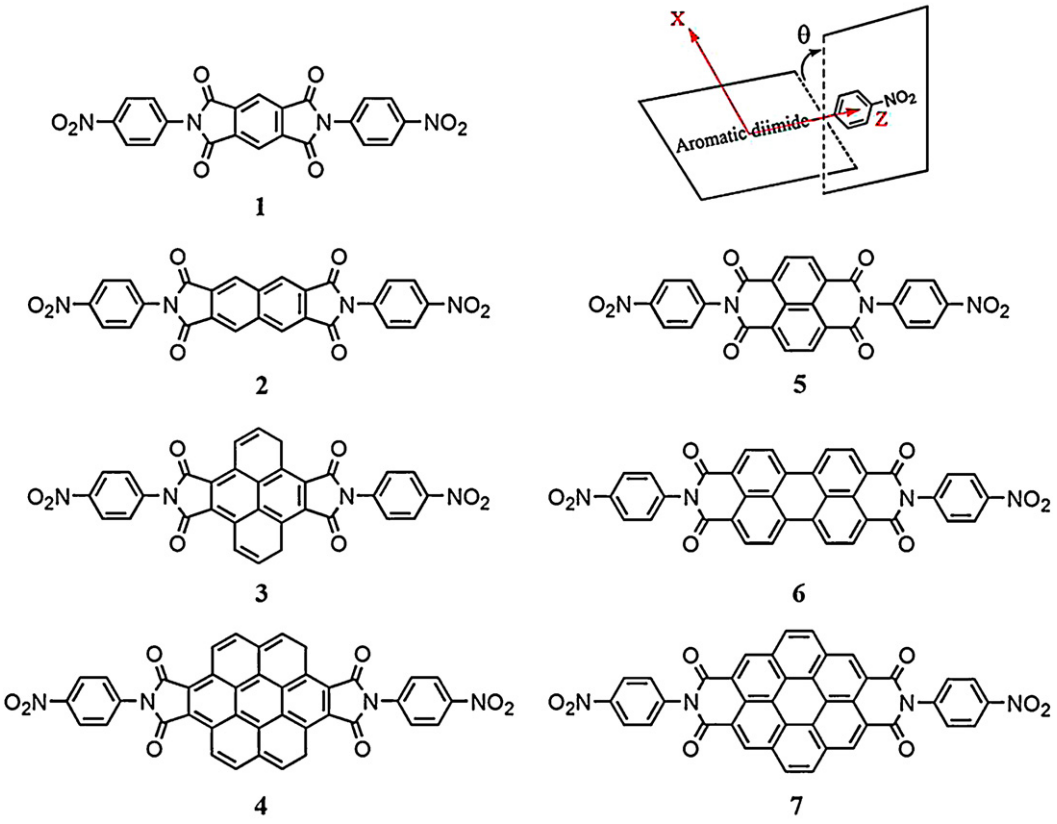

Scheme 1. Structures of the systems used in this study.

mechanism is important because this stability can be used to switch from one configuration to the other using a simply controlled, high-speed switching mechanism. Specific mechanisms, including oxidation/reduction [27], protonation/deprotonation [28] and photocyclization [29], have been used to switch NLO properties. In particular, reversible redox is an interesting way to control the NLO response of a molecule because the redox process can alter the donor/acceptor ability [30]. Pyromellitic diimides, naphthalene diimides and perylene diimides have been shown to undergo reversible one-electron reduction at modest potentials to form stable radical anions [31]. It is well known that open-shell systems can exhibit very large γ values, and recent studies have shown that the formation of radical systems during the redox process can enhance the NLO properties because of the delocalization of the frontier molecular orbitals [32,33]. Thus, large NLO responses are expected to be produced by one-electron reduction of aromatic diimide systems. Many researchers have studied the redox switching of the first hyperpolarizability theoretically and experimentally, but the switchable of the second hyperpolarizability has rarely been reported.

In this paper, we have investigated the effect of the aromatic core size along the perpendicular and longitudinal direction on the second hyperpolarizabilities of aromatic diimide systems. Moreover, the NLO switching of reduced form radical anions **1**$^{\bullet-}$, **5**$^{\bullet-}$ and **6**$^{\bullet-}$, obtained by a reversible redox process, has also been studied.

2. Computational details

The geometries of all of the systems were fully optimized at the (U)B3LYP/6-31+G(d,p) level [34–40]. The frequency calculations were performed at the same level because the geometry of each molecule was considered stable only when the molecule had no imaginary vibrational frequencies.

It is well known that time-dependent density functional theory (TDDFT) is one of the most reliable calculation methods for many applications [41], especially for the calculation of excitation energy in quantum chemistry, due to its efficiency and accuracy [42]. The absorption spectrum of system **5** has been measured experimentally in an o-dichlorobenzene solution, and the system showed one absorption band at 390 nm [43]. The TD-PBE0 functional improves the accuracy of excitation energies and charge-transfer bands for organic molecules [44–46]. Thus, we selected the PBE0/6-31+G(d,p) level combined with the polarized continuum model (PCM) [47] in an o-dichlorobenzene solution to simulate the absorption spectrum of system **5**. The calculated result shows an absorption band at 376.5 nm for system **5**. This calculated value is in reasonable agreement with the experimental value. Consequently, the absorption spectra of systems **1**–**7** were calculated at the PBE0/6-31+G(d,p) level in an o-dichlorobenzene solution.

The finite field (FF) approach is widely used to calculate NLO coefficients [48]. With a static electric field, the electric properties can be described by a Taylor's expansion of the energy, as shown in Eq. (1) [49]:

$$E = E^{(0)} - \mu_i F_i - \alpha_{ij} F_i F_j - \beta_{ijk} F_i F_j F_k - \gamma_{ijkl} F_i F_j F_k F_l - \cdots \quad (1)$$

where $E^{(0)}$ is the molecular energy in the absence of the applied electric field; μ_i is the molecular permanent dipole moment along the ith direction; F_i is the ith Cartesian component of the applied electric field; α, β and γ are the linear, first, and second hyperpolarizability tensors, respectively; and i, j, and k designate the different components along the x, y and z directions, respectively.

The polarizabilities α and the static second hyperpolarizabilities γ values are calculated using BHandHLYP [50], M06-2X [51] and CAM-B3LYP [52] functionals with the same basis set used in geometry optimizations by adopting the finite field (FF) approach, which consists in the fourth-order differentiation of the energy

Table 1
The bond lengths (Å) and dihedral angles θ (°) between the aromatic diimide and the nitrobenzene of the studied systems.

System	**1**	**2**	**3**	**4**	**5**	**6**	**7**	**1**$^{\bullet-}$	**5**$^{\bullet-}$	**6**$^{\bullet-}$
C—N	1.4253	1.4240	1.4220	1.4214	1.4474	1.4461	1.4466	1.4058	1.4332	1.4341
θ	40.49	39.83	40.04	39.91	89.96	89.97	90.00	29.42	59.29	61.05

with respect to the applied external electric field F [53]. The power series expansion convention is chosen for defining α and γ [54]. We use 1-point procedure with field amplitude of 0.0 and 4-point procedure with field amplitudes of 0.0, 0.0005, 0.0010 and 0.0015 a.u. to achieve numerical stability for α and γ from the following equation, respectively:

$$\alpha_{ij} = \frac{E(F) - 2E(0) + E(-F)}{(F)^2} \quad (2)$$

and

$$\gamma_{ijkl} = \frac{1}{36(F)^4}\{E(3F) - 12E(2F) + 39E(F) - 56E(0) + 39E(-F) - 12E(-2F) + E(-3F)\} \quad (3)$$

where $E(F)$ indicates the total energy in the presence of field F (applied in the different direction).

For a molecule, the average values of polarizability and the second hyperpolarizability are defined as follows:

$$\alpha = \frac{\alpha_{xx} + \alpha_{yy} + \alpha_{zz}}{3} \quad (4)$$

$$\gamma = \frac{1}{5}\{\gamma_{xxxx} + \gamma_{yyyy} + \gamma_{zzzz} + 2[\gamma_{xxyy} + \gamma_{xxzz} + \gamma_{yyzz}]\} \quad (5)$$

All of the calculations were performed using the GAUSSIAN 09W program package [55]. The density of states (DOS) was calculated using the Aomix program [56].

3. Results and discussion

3.1. Geometric structure

The geometric structures of systems **1**–**7** with all real frequencies were obtained using the B3LYP/6-31+G(d,p) level, as shown in Scheme 1. The structures of systems **1**–**7** have C_{2h} symmetry. The aromatic diimides of all of the systems lie in the xz plane, with their longitudinal axis along the z direction. The key geometric parameters are listed in Table 1. The lengths of the C—N bonds between the aromatic diimides and the nitrobenzene of systems **1**–**4** are smaller than those of systems **5**–**7**. Additionally, the dihedral angles (θ) of systems **1**–**4**, which are formed by the aromatic diimides and the nitrobenzene (see Scheme 1), are 40.49°, 39.83°, 40.04° and 39.91°, whereas those of systems **5**–**7** are almost right angles. Grucela-Zajac et al. also studied the dihedral angles between the acridine ring and the imide-based compounds [57]. The result shows that the dihedral angle value is 61.20° in the five-membered imide system, whereas imide moieties are perpendicular to the acridine ring in six-membered imide systems, which is in line with the situation of the above mentioned. This phenomenon may be due to the larger steric repulsion between the oxygen atom of the six-membered aromatic diimides and the hydrogen atom of the nitrobenzene. As an example, we further assess the obtained potential energy surfaces for the five-membered aromatic diimide system **2** and the six-membered aromatic diimide system **5** using single point calculations based on the optimized geometries along the torsion angle for θ from 0° to 90° with increments of 15° (Fig. 1). Systems **2** and **5** were the most stable when θ was 39.83° and 89.96°, respectively. These structural changes must affect the molecular NLO properties.

3.2. Polarizabilities

The α_{xx}, α_{yy}, α_{zz} and α values of all systems at different functionals are given in Table 2. As shown in Table 2, the α_{zz} value is the largest among all the components, because the skeleton atoms mostly located on the z axis. In the five-membered aromatic diimide systems **1**–**4**, the order of polarizability values: **4** > **3** > **2** > **1** is consistent in different functionals. This indicates that the size of systems has influence on the polarizability, and the α value increases with the increasing size of the molecular geometry. Similar results are observed for the six-membered aromatic diimide systems **5**–**7**, in which the order of polarizability values: **7** > **6** > **5**.

3.3. Static second hyperpolarizabilities

3.3.1. The effect of the aromatic core size on the second hyperpolarizabilities

The calculated second hyperpolarizabilities and their components for systems **1**–**7** are listed in Table 3. To investigate the influence of the DFT methods on the NLO responses, the γ values were calculated using the BHandHLYP, M06-2X and CAM-B3LYP functionals based on the same geometries. The results show that the γ values obtained using different functionals are very close for the same system, and the three functionals display the same

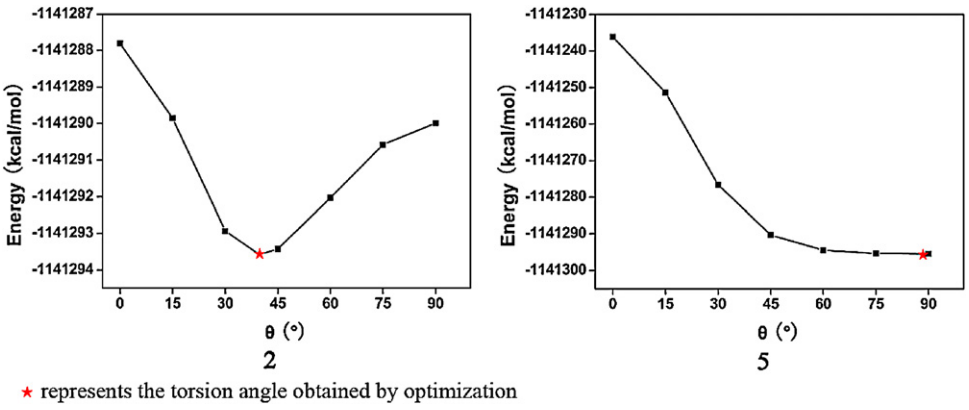

Fig. 1. Potential energy surfaces of systems **2** and **5** along the torsion angle θ.

Table 2
Computed polarizabilities (1×10^{-24} esu) of the neutral systems **1**–**7** using different functionals.

System	Functional	α_{xx}	α_{yy}	α_{zz}	α
1	BhandHLYP	40.87	25.91	79.07	48.62
	M06-2X	41.28	25.95	79.83	49.02
	CAM-B3LYP	41.49	26.19	80.70	49.46
2	BhandHLYP	46.34	28.73	103.94	59.67
	M06-2X	46.89	28.75	104.77	60.14
	CAM-B3LYP	47.05	29.02	105.69	60.59
3	BhandHLYP	68.51	32.47	105.06	68.68
	M06-2X	68.61	32.43	106.39	69.14
	CAM-B3LYP	68.99	32.76	106.98	69.57
4	BhandHLYP	81.81	37.23	146.85	88.63
	M06-2X	82.32	37.15	147.86	89.11
	CAM-B3LYP	82.46	37.54	148.72	89.57
5	BhandHLYP	42.90	36.58	86.12	55.20
	M06-2X	43.28	36.80	86.43	55.51
	CAM-B3LYP	43.52	36.91	87.56	56.00
6	BhandHLYP	59.89	43.05	146.86	83.27
	M06-2X	60.43	43.21	145.80	83.15
	CAM-B3LYP	60.62	43.41	147.79	83.94
7	BhandHLYP	73.61	45.08	141.89	86.86
	M06-2X	74.14	45.22	142.50	87.29
	CAM-B3LYP	74.29	45.45	143.65	87.79

trends in the γ values for the studied systems. To discuss these results in more detail, we use the data from the BHandHLYP functional to evaluate the order of the γ values for all of the systems. As mentioned earlier, the γ_{zzzz} value is clearly larger than the other components due to the molecular coordinates. Hence, the major contribution to the γ value is the γ_{zzzz} component. In the five-membered aromatic diimide systems **1**–**4**, the γ_{zzzz} value of system **2** is larger than that of system **1** due to the increase in the number of benzenes along the longitudinal direction as compared with system **1**, which results in an increase in the γ value of system **2**, ~1.8 times larger than that of system **1**. Based on the geometry of system **2**, system **3** has two more benzenes along the *x* axis, i.e., the aromatic core changes into pyrene, and its γ value decreases. From the values listed in Table 3, the γ_{zzzz} value of system **3** is 705.42×10^{-36} esu, which is less than that of system **2**, whereas the γ_{xxxx} and γ_{xxzz} values increase. This phenomenon may occur because the increased number of benzenes in the *x* direction weakens the charge transfer ability along the *z*-axis. The γ value of system **4** is 331.85×10^{-36} esu, which has one and two more benzenes along the *z* and *x* directions, respectively, compared with system **3**. The γ_{zzzz} value of system **4** is ~2.0 times larger than that of system **3**, and the γ_{xxxx} and γ_{xxzz} values increase to 50.20×10^{-36} esu and 74.53×10^{-36} esu, respectively, whereas the other components change slightly. There is an order to the γ values: **4** > **2** > **3** > **1**.

Similar results are observed for the six-membered aromatic diimide systems **5**–**7**. System **6** has the largest γ value, which are ~4.5 and ~1.5 times larger than those of systems **5** and **7**, respectively, because the number of benzenes is more than that of system **5** along the *z* axis and less than that of system **7** along the *x* axis. The observed differences in the second hyperpolarizabilities calculated at the DFT level for the different systems are mainly caused by the longitudinal component along the *z* axis. The γ_{zzzz} value of system **6** is significantly larger than those of systems **5** and **7**; thus, the calculated γ values of systems **5**–**7** are as follows: **6** > **7** > **5**. This result indicates that the γ values of the studied systems are more sensitive to the number of benzenes along the *z* axis than to the number of benzene rings along the *x* axis, that is, the introduction of benzenes increases the degree of charge transfer along the longitudinal direction and enhances the molecular NLO responses.

Table 3
Computed second hyperpolarizabilities (1×10^{-36} esu) of the neutral systems **1**–**7** using different functionals.

System	Functional	γ_{xxxx}	γ_{yyyy}	γ_{zzzz}	γ_{xxyy}	γ_{xxzz}	γ_{yyzz}	γ
1	BhandHLYP[a]	11.67	13.24	469.83	2.99	14.25	2.92	107.01
	BhandHLYP[b]	11.08	12.15	480.64	2.81	13.78	2.59	108.45
	M06-2X	10.99	11.98	483.34	2.87	14.58	3.02	109.45
	CAM-B3LYP	12.67	13.86	483.96	3.27	14.84	3.28	110.65
2	BhandHLYP[a]	16.02	15.07	861.78	3.80	15.97	3.72	187.97
	BhandHLYP[b]	15.10	13.86	878.67	3.57	15.48	3.31	190.47
	M06-2X	15.29	13.48	880.13	3.63	16.59	3.88	191.42
	CAM-B3LYP	17.18	15.60	868.98	4.12	16.48	4.13	190.25
3	BhandHLYP[a]	20.97	17.20	705.42	7.02	65.26	4.26	179.34
	BhandHLYP[b]	18.83	16.04	715.07	6.73	63.09	3.89	179.47
	M06-2X	23.77	15.36	699.80	6.29	63.33	4.40	177.39
	CAM-B3LYP	24.86	17.79	711.81	7.44	67.06	4.74	182.59
4	BhandHLYP[a]	50.20	19.48	1412.04	8.37	74.53	5.87	331.85
	BhandHLYP[b]	47.37	18.24	1421.11	7.93	72.23	5.30	331.53
	M06-2X	48.97	17.46	1395.26	7.48	71.59	5.90	326.32
	CAM-B3LYP	51.83	20.11	1407.93	8.62	73.68	6.46	331.48
5	BhandHLYP[a]	20.20	11.45	228.69	6.19	5.35	2.61	57.72
	BhandHLYP[b]	19.07	10.46	228.79	5.76	4.85	2.40	56.87
	M06-2X	19.27	10.85	235.10	5.48	6.77	3.10	59.19
	CAM-B3LYP	20.56	12.39	246.83	6.37	6.57	3.24	62.43
6	BhandHLYP[a]	29.80	14.95	1236.10	8.51	0.55	5.23	261.88
	BhandHLYP[b]	27.89	13.80	1227.29	8.03	-0.88	4.88	258.61
	M06-2X	28.34	14.07	1362.40	7.55	5.30	5.85	288.44
	CAM-B3LYP	30.38	16.05	1364.76	8.67	3.93	5.91	289.64
7	BhandHLYP[a]	62.17	15.74	706.74	9.69	20.10	4.55	170.66
	BhandHLYP[b]	59.35	14.60	704.60	9.25	19.15	4.40	168.83
	M06-2X	59.10	14.82	712.99	8.63	22.35	5.03	171.79
	CAM-B3LYP	61.66	16.68	733.93	10.12	21.95	5.74	177.58

[a] BhandHLYP/6-31+G(d,p).
[b] BhandHLYP/6-311+G(d,p).

Interestingly, systems **2** and **5** have the same aromatic hydrocarbon in different arrangements. However, the large difference in the γ_{zzzz} values results in the γ value of system **2** being ~3.3 times larger than that of system **5**. Similar results are observed for systems **4** and **7**, in which system **4** has the larger γ value. The distance of the charge transfer along the z axis plays an important role in the second hyperpolarizabilities. Consequently, the NLO responses of the aromatic diimide molecules can be tuned by increasing the size of the aromatic core, especially along the z direction.

We have also calculated the γ values of systems **1**–**7** using the 6–311+G(d,p) basis at BHandHLYP level to check the effects of the triplet-ζ basis set on NLO responses. The results show that the larger 6-311+G(d,p) basis set has a little influence on the γ values of systems **1**–**7** compared with the 6–31+G(d,p) basis set.

To gain an intuitive understanding of the static second hyperpolarizability origin, Dirk et al. [58] established a simple link between the γ value and a low-lying charge-transfer transition using the three-level model, and the physical quantities in the three-level model may help to qualitatively understand the variations in the γ value. For the studied centrosymmetric systems, the second hyperpolarizability is proportional to the second power of the transition moment μ_{gm} and inversely proportional to the third power of the transition energy E_{gm}, according to the three-level expression. μ_{gm} and E_{gm} are the major factors that determine the γ value. The transition energies, transition moments, and relevant orbital transitions of the crucial excited states obtained at the TD-PBE0/6-31+G(d,p) level are listed in Table 4. In this paper, the factor μ_{gm}^2/E_{gm}^3 was used to roughly estimate the γ value and is also listed in Table 4. As shown in Table 4, the order of the μ_{gm}^2/E_{gm}^3 values of systems **1**–**4** are **4** > **2** > **3** ≈ **1**, whereas the order of the γ values is **4** > **2** > **3** > **1**. This ordering may be due to other factors that influence the γ values of systems **1** and **3** (discussed later). For the six-membered aromatic diimide systems, the order of the μ_{gm}^2/E_{gm}^3 values of systems **5**–**7** are **6** > **7** > **5**, and the order of the γ values is consistent with this order values. Moreover, the μ_{gm}^2/E_{gm}^3 value of system **2** is larger than that of system **5**, which has the same aromatic hydrocarbon in a different arrangement, resulting in a larger γ value for system **2**. This result is similar to that for systems **4** and **7**, with system **4** having the larger γ value.

To gain more insight into the NLO responses of systems **1** and **3**, we analyzed the orbital transition properties that involved the crucial excited states. The molecular orbital plots of systems **1** and **3** are depicted in Fig. 2 based on the TDDFT results. For a better understand the electron density of the corresponding molecular orbitals, the Mulliken population analyses on the studied systems have been provided in Table S1 of Supporting Information. Combine Fig. 2 with Table S1, the HOMO-8 and HOMO-9 of system **1** mainly center on the nitro groups on both sides of the molecule and contain some contributions from the adjacent benzene ring (98% for HOMO-8 and 94% for HOMO-9). The HOMO and HOMO-1 of system **1** localize on the nitrobenzene (66% for HOMO and 68% for HOMO-1) and diimide (22% for HOMO and 24% for HOMO-1), and some electron density is localized on the aromatic core (8%) in the HOMO. The LUMO + 1 of system **1** distributes over the whole molecule, whereas the LUMO + 2 localizes on the nitrobenzene (96%). Combining these results with the data in Table 4, it can be determined that the electron transition of system **1** mainly arises from the HOMO → LUMO + 1 (69%) and the HOMO-1 → LUMO + 2 (13%) excited states, i.e., the charge transfer occurs from the aromatic diimides nitrobenzene and diimide to the nitrobenzene and from the diimide to the nitrobenzene. For system **3**, the HOMO-3 and HOMO-2 are mainly located on the nitrobenzene (62% for HOMO-3 and 66% for HOMO-2) and diimide (22% for HOMO-3 and 20% for HOMO-2), with some contributions from the aromatic core (8% for HOMO-3 and 4% for HOMO-2), whereas the HOMO localizes on the aromatic core (84%) and the nitrogen atom of the diimide (6%). The LUMO + 2 and LUMO + 3 have similar electron density distributions that center on the nitrobenzene (86%), and the LUMO + 4 is located on the aromatic core (86%). Moreover, the crucial excited states of system **3** are HOMO-2 → LUMO + 3 (41%), HOMO → LUMO + 4 (32%) and HOMO-3 → LUMO + 2 (19%). These excitations can be assigned to the π→π* transition of the aromatic diimides and to the charge transfer patterns from the aromatic core and the diimide to the nitrobenzene along the z axis, which contribute to the γ value. The analysis shows that the degree of charge transfer for system **3** is larger than that of system **1**. Therefore, the γ value of system **3** is larger than that of system **1**.

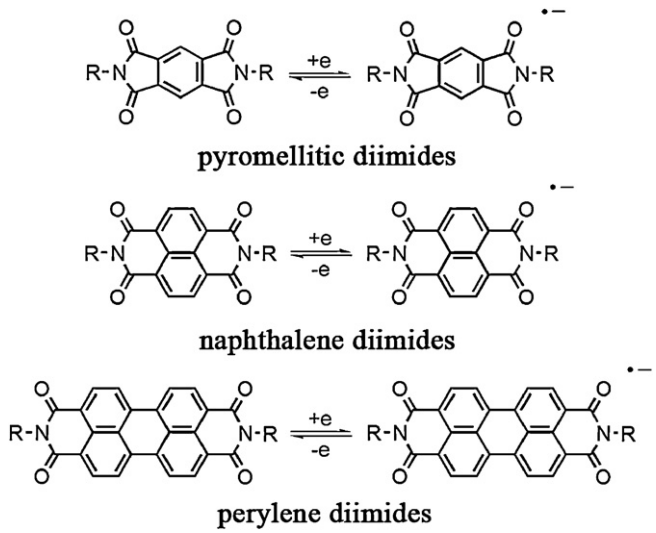

Scheme 2. Reversible redox processes of pyromellitic diimides, naphthalene diimides and perylene diimides.

We also considered the electron transitions of the five-membered aromatic diimide system **4** and the six-membered aromatic diimide system **7**, which possess the same aromatic hydrocarbon in different arrangements. Fig. 3 shows the frontier molecular orbitals of systems **4** and **7** associated with the dominant excited states. The Mulliken population analyses of the corresponding molecular orbitals have been supplemented in Table S1 of Supporting Information. For system **4**, the electron density is mainly located on the aromatic diimide (84%) in the HOMO-1, whereas the electron density localizes almost completely on the nitrobenzenes (94%) on both sides of the molecule in the LUMO + 1. The large difference in the electron distributions of the HOMO-1 and LUMO + 1 generates an obvious charge transfer from the aromatic diimide to the nitrobenzene, which leads to the large NLO response. The HOMOs and LUMOs of system **7** have similar delocalizations, which are all located on the aromatic diimide, except for the N atom. Hence, the crucial electron excitation can be attributed to the π→π* transition of the aromatic diimides. The difference in the charge transfer patterns of systems **4** and **7** may be due to their different structures. As previously mentioned, the dihedral angles θ of systems **4** and **7** are 39.91° and 90.00°, respectively; thus, a smaller θ is beneficial to the electron transition between the aromatic diimide and the nitrobenzene for system **4**, which should enhance the NLO response.

3.3.2. *The effect of redox switching on the NLO responses*

Aromatic diimides typically undergo reversible one-electron reductions that yield corresponding radical anions, and pyromellitic diimides, naphthalene diimides and perylene diimides have been experimentally shown to be redox-active units [31,59,60] (Scheme 2). Thus, we used systems **1**, **5** and **6** to determine the effect of redox on the static second hyperpolarizabilities of the

Table 4
TDDFT calculations of the studied systems.

System	E_{gm} (eV)	μ_{gm}^2	Excited state contributions	μ_{gm}^2/E_{gm}^3
1	3.96	12.4680	HOMO → LUMO + 1 (69%) HOMO-1 → LUMO + 2 (13%) HOMO-8 → LUMO + 2 (6%) HOMO-9 → LUMO + 1 (6%)	0.2008
2	3.82	21.3891	HOMO-1 → LUMO + 1 (69%) HOMO-2 → LUMO + 2 (15%) HOMO-8 → LUMO + 2 (6%)	0.3837
3	4.07	13.2446	HOMO-2 → LUMO + 3 (41%) HOMO → LUMO + 4 (32%) HOMO-3 → LUMO + 2 (19%)	0.1965
4	3.28	15.9135	HOMO-1 → LUMO + 1 (90%)	0.4510
5	4.53	6.4712	HOMO-4 → LUMO + 2 (48%) HOMO-5 → LUMO + 1 (46%)	0.0696
6	2.29	19.3885	HOMO → LUMO (100%)	1.6144
7	3.86	14.3854	HOMO → LUMO + 3 (91%) HOMO-1 → LUMO (5%)	0.2501

aromatic diimide systems. The geometries of the reduced form radical anions $\mathbf{1}^{\bullet-}$, $\mathbf{5}^{\bullet-}$ and $\mathbf{6}^{\bullet-}$ were optimized at the UB3LYP/6-31+G(d,p) level. The lengths of the C—N bonds and dihedral angles θ of radical anions $\mathbf{1}^{\bullet-}$, $\mathbf{5}^{\bullet-}$ and $\mathbf{6}^{\bullet-}$ were listed in Table 1. As shown in Table 1, the bond distance shortens and the θ decreases through one-electron reduction for systems $\mathbf{1}^{\bullet-}$, $\mathbf{5}^{\bullet-}$ and $\mathbf{6}^{\bullet-}$. These changes on structure must affect the molecular NLO properties. We also studied the reduced centers. It is well known that changes in the electronic properties during the redox process are closely related to the nature of the frontier molecular orbitals. Fig. 4 shows the lowest unoccupied molecular orbital LUMOs for the studied neutral parents. For all of the neutral forms, the LUMOs are entirely delocalized on the aromatic diimides. This result indicates that the aromatic diimides will be the reduced centers. This idea was supported by the spin density distributions of $\mathbf{1}^{\bullet-}$, $\mathbf{5}^{\bullet-}$ and $\mathbf{6}^{\bullet-}$ (Fig. 4). The reduction may affect the geometry of the reduced center and alter the electronic structure features, and thus, the γ values of systems **1**, **5** and **6** might change during the redox process.

To further investigate the electronic structures of the neutral forms and their reduced radical anions, total density of state (TDOS) and projected partial density of state (PDOS) calculations were performed using the Aomix program. As shown in Fig. 5, the aromatic diimide moieties provide almost the entire contribution to the LUMO formation of the neutral systems **1**, **5** and **6**, and there are identical contributions to the α-HOMO for the corresponding radical anions $\mathbf{1}^{\bullet-}$, $\mathbf{5}^{\bullet-}$ and $\mathbf{6}^{\bullet-}$, which is in line with the electronic distribution of α-HOMO for the system as the reference 57 mentioned. This result also demonstrates that the aromatic diimide moieties are the reduced centers of the studied systems, which is in good agreement with the conclusion mentioned above. Interestingly, it is observed that the distribution of the DOS is very similar for the neutral parent and its radical anion for systems **1** and **5**. As shown in Fig. 5, the aromatic diimide contributes little to the

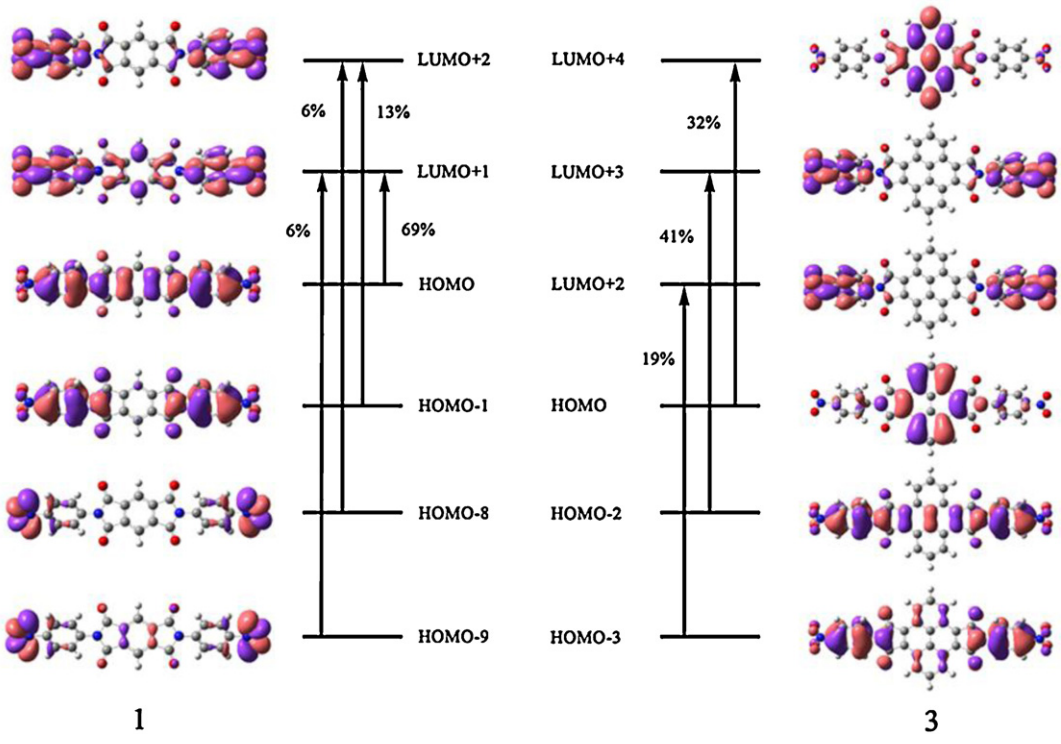

Fig. 2. Frontier molecular orbitals of systems **1** and **3** that are involved in the dominant electron transitions.

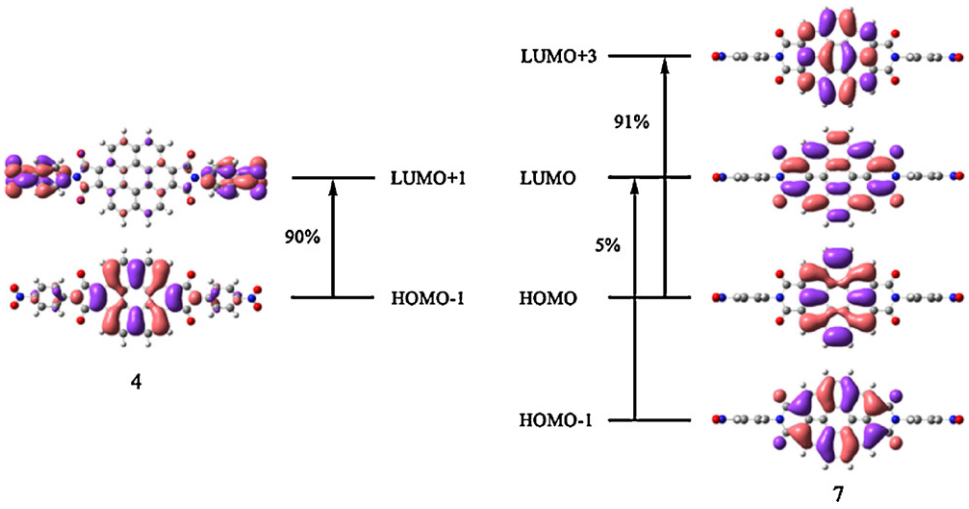

Fig. 3. Frontier molecular orbitals of systems **4** and **7** that are involved in the dominant electron transitions.

HOMOs in neutral parents **1** and **5**, whereas it plays a significant role in the formation of the α-HOMOs for radical anions **1**$^{\bullet-}$ and **5**$^{\bullet-}$. It comes from the enhancement of electronic donating ability for the aromatic diimide after the injection of an extra electron to form the radical anion. For system **6**, which has a large aromatic core, the aromatic diimide is a large portion of the HOMOs for both forms. The LUMO centers on the aromatic diimide, whereas the nitrobenzene mainly contributes to the other LUMOs for the neutral parent. In radical anion **6**$^{\bullet-}$, the aromatic diimide contributes little to the α-LUMO and α-LUMO + 1 and mostly contributes to the α-LUMO + 2. For a clearly insight on the charge transfer of systems **6** and **6**$^{\bullet-}$, the frontier molecular orbital was presented in Fig. S1 of Supporting Information. The analysis illustrates that there are $\pi \rightarrow \pi^*$ transitions in the aromatic diimide for system **6**, whereas a charge transfer from the aromatic diimide to the nitrobenzene occurs in radical anion **6**$^{\bullet-}$. The difference in the charge transfer direction may lead to a change in the second hyperpolarizability of system **6**$^{\bullet-}$. The changing electron structure during the redox process could influence the NLO responses.

As mentioned above, the static second hyperpolarizabilities of the neutral forms are calculated with three different DFT functionals, and the results exhibit good consistency. Moreover, the BHandHLYP method has been widely used to calculate the static second hyperpolarizabilities of radicals and radical ions by Nakano et al. [61–63]. Therefore, the γ values of radical anions **1**$^{\bullet-}$, **5**$^{\bullet-}$ and **6**$^{\bullet-}$ have been calculated at the UBHandHLYP/6-31+G(d,p) level. The γ values and their components for radical anions **1**$^{\bullet-}$, **5**$^{\bullet-}$ and **6**$^{\bullet-}$ are shown in Table 5. The values listed in Table 5 indicate that the components of all of the radical anions change slightly compared with those of the corresponding neutral forms except for the γ_{zzzz} and γ_{xxzz} values. The γ_{xxzz} values of radical anions **1**$^{\bullet-}$, **5**$^{\bullet-}$ and **6**$^{\bullet-}$ are larger than those of their neutral systems, which is attributed to over-delocalization of the electron density in the *xz* plane after the injection of an electron to form the radical anions. The γ_{zzzz} value of 76.19×10^{-36} esu for **1**$^{\bullet-}$ is lower than that of system **1**, which results in a decrease in the γ value of **1**$^{\bullet-}$. Similarly, for radical anion **5**$^{\bullet-}$, the γ_{zzzz} value is significantly lower than that of system **5**, and the γ value of **5**$^{\bullet-}$ decreases. It is interesting to note that the sign of the γ_{zzzz} value of radical anion **6**$^{\bullet-}$ becomes negative, which must be related to the change in the charge transfer direction mentioned above, and that the absolute value of the γ_{zzzz} value is significantly larger than that of the neutral parent. Thus, the absolute value of the γ value of **6**$^{\bullet-}$ is ~7.3 times larger than that of system **6**. The results indicate that the reduction of systems **1** and **5**, which have small aromatic cores, cannot effectively enhance the second hyperpolarizability, whereas the redox process has a substantial influence on the second hyperpolarizability of system **6,** which has a large aromatic core, because the electrons could extensively delocalize on the aromatic diimides after the injection of an electron to form the radical anion. Therefore, system **6** is a more promising redox-switchable NLO molecular material.

It is well known that Bond Length Alternation (BLA) is an important parameter that affects the NLO properties of linear conjugated organic molecules [11]. Recently, Ottonelli et al. [64] adopted the BLA definition generally used for polycyclic aromatic hydrocarbons

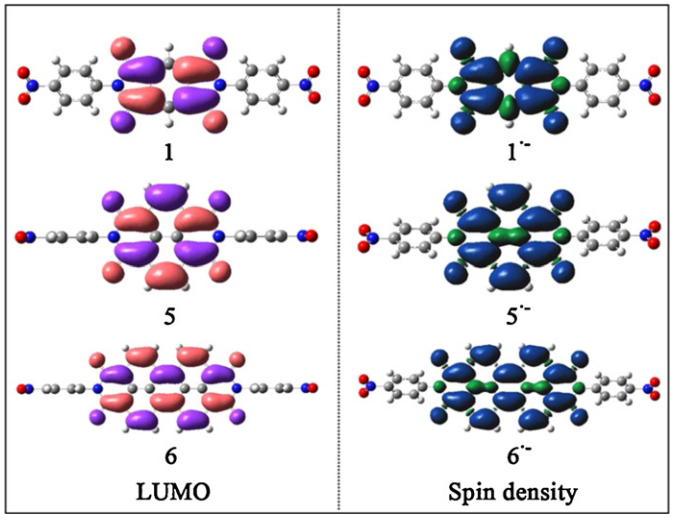

Fig. 4. LUMOs of the neutral systems **1**, **5** and **6**, and the spin density plots of the corresponding reduced systems **1**$^{\bullet-}$, **5**$^{\bullet-}$ and **6**$^{\bullet-}$.

Table 5
Second hyperpolarizabilities (1×10^{-36} esu) of the reduced radical anions.

System	γ_{xxxx}	γ_{yyyy}	γ_{zzzz}	γ_{xxyy}	γ_{xxzz}	γ_{yyzz}	γ
1$^{\bullet-}$	11.47	16.01	76.19	4.95	151.44	3.70	84.77
5$^{\bullet-}$	−19.21	18.72	17.36	12.02	87.99	2.17	44.25
6$^{\bullet-}$	17.75	22.55	−9725.67	16.51	59.20	0.20	−1906.71

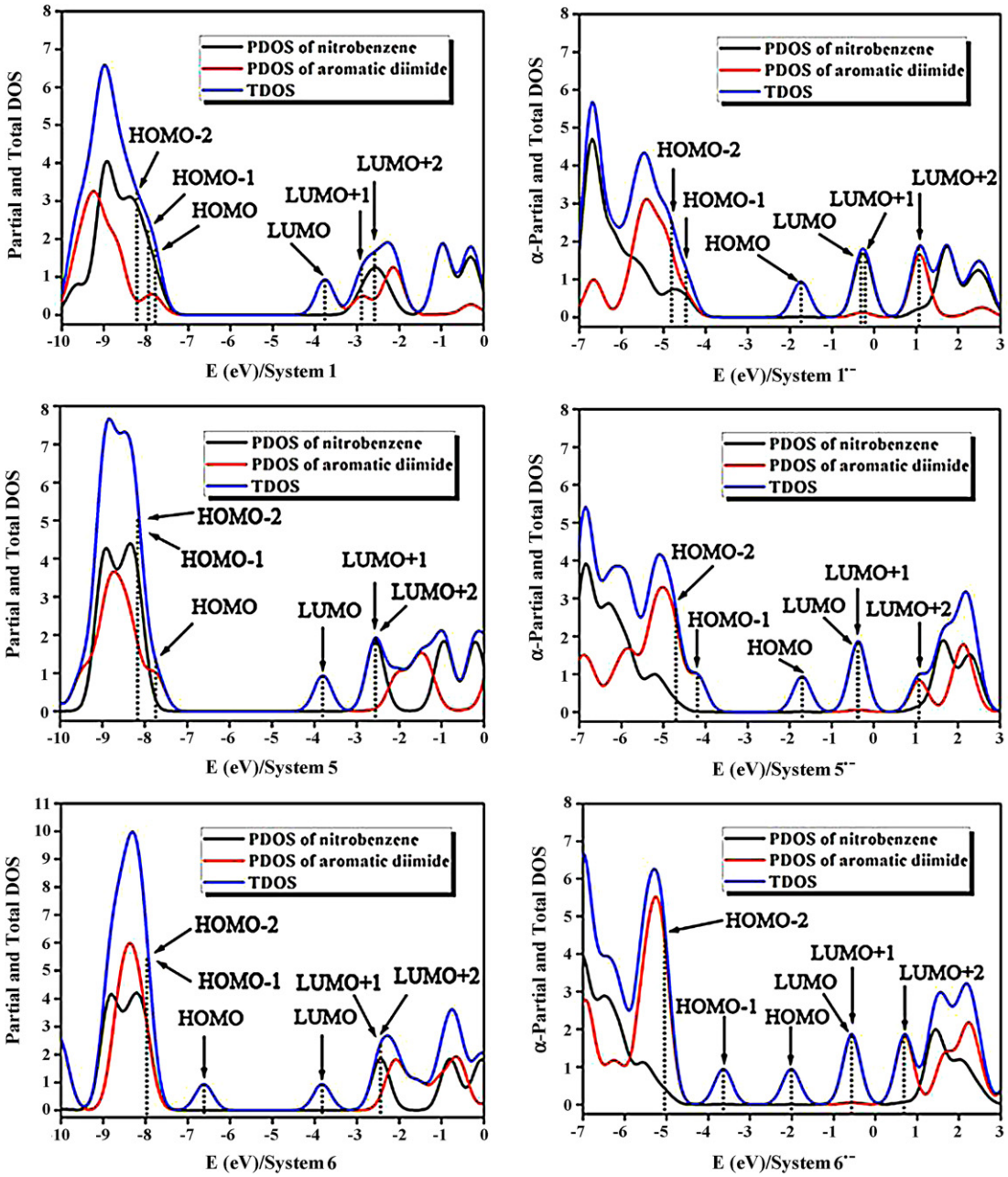

Fig. 5. Partial and total density of states (PDOS and TDOS) for all of the redox systems.

(PAHs), which is correlated to the aromaticity index, i.e., the standard deviations in the C—C ring bonds:

$$\mathrm{BLA} = \sqrt{\frac{1}{N}\sum_{i}(d_i - d_M)^2} \qquad (6)$$

Here, N is the total number of C—C bonds, d_i is the ith bond length, and d_M is the mean C—C bond length. The BLA values of the aromatic cores for the neutral parents and the reduced radical anions are listed in Table 6. An analysis of the data in Table 6 shows that the BLA values of radical anions **1**•− and **5**•− are larger than those of the corresponding neutral systems. This result implies that the aromaticities of systems **1**•− and **5**•− are weaker than those of **1** and **5**, and thus, radical anions **1**•− and **5**•− exhibit smaller γ values. Compared with neutral **6**, the decrease in the BLA value of radical anion **6**•− shows that more C—C bonds are involved with the change in their bond order and that the delocalization pathway is increased. Hence, the γ value of radical anion **6**•− is larger than that of the neutral form. Overall, the BLA value is a crucial factor that affects the second hyperpolarizabilities of the studied redox systems.

Table 6
BLA values of the neutral parents and their reduced radical anions.

System	**1**	**1**•−	**5**	**5**•−	**6**	**6**•−
BLA (neutral)	0.0026	–	0.0145	–	0.0240	–
BLA (reduced)	–	0.0196	–	0.0148	–	0.0200

4. Conclusions

We investigated the NLO properties of two types of systems containing aromatic diimides for the first time: the five-membered aromatic diimide system and the six-membered aromatic diimide system. DFT-FF calculations indicate that the size of the aromatic core can affect the second hyperpolarizability. Particularly, the γ values of the studied systems are more sensitive to the number of benzenes along the longitudinal axis than to the number of benzene rings along the perpendicular axis, that is, the introduction of benzenes increases the degree of charge transfer along the longitudinal direction and enhances the γ values. Interestingly, for systems **2** and **5,** which have the same aromatic hydrocarbon in different arrangements, the γ value of system **2** is larger than that of system **5** due to a wide charge transfer along the longitudinal axis. The same result is observed for systems **4** and **7**, in which system **4** possesses the larger γ value. Moreover, the third-order NLO responses of the reduced form radical anions $\mathbf{1}^{\bullet-}$, $\mathbf{5}^{\bullet-}$and $\mathbf{6}^{\bullet-}$, obtained by a reversible redox process, have been examined. The results show that the redox significantly affects the geometric structures, resulting in a change in the BLA values of the aromatic cores. The BLA value of radical anion $\mathbf{6}^{\bullet-}$ is small with respect to that of its neutral parent. This result implies that the conjugation of radical anion $\mathbf{6}^{\bullet-}$ is enhanced after the injection of an electron, which leads to the large γ value (-1906.71×10^{-36} esu). It is worth noting that the sign of the γ value changes from positive to negative during the redox process because of the different charge transfer directions of the reduced form of the radical anion and the neutral parent. Therefore, system **6**, which has a large aromatic core, could be an excellent redox-switchable NLO material.

Acknowledgments

The authors gratefully acknowledge the financial support of the Natural Science Foundation of China (No. 21173035) and the Natural Science Foundation of Jilin province (No. 20101154).

Appendix A. Supplementary data

Supplementary data associated with this article can be found, in the online version, at http://dx.doi.org/10.1016/j.jmgm.2013.01.008.

References

[1] J.L. Brédas, C. Adant, P. Tackx, A. Persoons, B.M. Pierce, Third-order nonlinear optical response in organic materials: theoretical and experimental aspects, Chemical Reviews 94 (1994) 243–278.
[2] V.M. Geskin, C. Lambert, J.L. Brédas, Origin of high second- and third-order nonlinear optical response in ammonio/borato diphenylpolyene zwitterions: the remarkable role of polarized aromatic groups, Journal of the American Chemical Society 125 (2003) 15651–15658.
[3] B. Kirtman, B. Champagne, D.M. Bishop, Electric field simulation of substituents in donor–acceptor polyenes: a comparison with Ab Initio predictions for dipole moments, polarizabilities, and hyperpolarizabilities, Journal of the American Chemical Society 122 (2000) 8007–8012.
[4] M. Nakano, T. Minami, K. Yoneda, S. Muhammad, R. Kishi, Y. Shigeta, T. Kubo, L. Rougier, B. Champagne, K. Kamada, K. Ohta, Giant enhancement of the second hyperpolarizabilities of open-shell singlet polyaromatic diphenalenyl diradicaloids by an external electric field and donor–acceptor substitution, The Journal of Physical Chemistry Letters 2 (2011) 1094–1098.
[5] W.H. Zhou, S.M. Kuebler, K.L. Braun, T. Yu, J.K. Cammack, C.K. Ober, J.W. Perry, S.R. Marder, An efficient two-photon-generated photoacid applied to positive-tone 3D microfabrication, Science 296 (2002) 1106–1109.
[6] P.K. Frederiksen, M. Jørgensen, P.R. Ogilby, Two-photon photosensitized production of singlet oxygen, Journal of the American Chemical Society 123 (2001) 1215–1221.
[7] Z.B. Cai, M. Zhou, J.H. Xu, Degenerate four-wave mixing determination of third-order optical nonlinearities of three mixed ligand nickel(II) complexes, Journal of Molecular Structure 1006 (2011) 282–287.
[8] H.S. Nalwa, Organic materials for third-order nonlinear optics, Advanced Materials 5 (1993) 341–358.
[9] H. Nagai, M. Nakano, K. Yoneda, H. Fukui, T. Minami, S. Bonness, R. Kishi, H. Takahashi, T. Kubo, K. Kamada, K. Ohta, B. Champagne, E. Botek, Theoretical study on third-order nonlinear optical properties in hexagonal graphene nanoflakes: edge shape effect, Chemical Physics Letters 477 (2009) 355–359.
[10] D. Beljonne, Z. Shuai, J.L. Brédas, Theoretical study of thiophene oligomers: electronic excitations, relaxation energies, and nonlinear optical properties, Journal of Chemical Physics 98 (1993) 8819–8828.
[11] F. Meyers, S.R. Marder, B.M. Pierce, J.L. Brédas, Electric field modulated nonlinear optical properties of donor–acceptor polyenes: sum-over-states investigation of the relationship between molecular polarizabilities (α, β, and γ) and bond length alternation, Journal of the American Chemical Society 116 (1994) 10703–10714.
[12] M. Nakano, H. Fujita, M. Takahata, K. Yamaguchi, Theoretical study on second hyperpolarizabilities of phenylacetylene dendrimer: toward an understanding of structure–property relation in NLO responses of fractal antenna dendrimers, Journal of the American Chemical Society 124 (2002) 9648–9655.
[13] M. Nakano, R. Kishi, K. Yoneda, Y. Inoue, T. Inui, Y. Shigeta, T. Kubo, B. Champagne, Third-order nonlinear optical properties of open-shell supermolecular systems composed of acetylene linked phenalenyl radicals, Journal of Physical Chemistry A 115 (2011) 8767–8777.
[14] G.P. Wiederrecht, M.P. Niemczyk, W.A. Svec, M.R. Wasielewski, Ultrafast photoinduced electron transfer in a chlorophyll-based triad: vibrationally hot ion pair intermediates and dynamic solvent effects, Journal of the American Chemical Society 118 (1996) 81–88.
[15] H. Levanon, T. Galili, A. Regev, G.P. Wiederrecht, W.A. Svec, M.R. Wasielewski, Determination of the energy levels of radical pair states in photosynthetic models oriented in liquid crystals with time-resolved electron paramagnetic resonance, Journal of the American Chemical Society 120 (1998) 6366–6373.
[16] M.A. Angadi, D. Gosztola, M.R. Wasielewski, Characterization of photovoltaic cells using poly(phenylenevinylene) doped with perylenediimide electron acceptors, Journal of Applied Physics 83 (1998) 6187–6189.
[17] G.P. Wiederrecht, M.R. Wasielewski, Photorefractivity in polymer-stabilized nematic liquid crystals, Journal of the American Chemical Society 120 (1998) 3231–3236.
[18] M.P. Debreczeny, W.A. Svec, E.M. Marsh, M.R. Wasielewski, Femtosecond optical control of charge shift within electron donor–acceptor arrays: an approach to molecular switches, Journal of the American Chemical Society 118 (1996) 8174–8175.
[19] S.K. Lee, Y. Zu, A. Herrmann, Y. Geerts, K. Müllen, A.J. Bard, Electrochemistry, spectroscopy and electrogenerated chemiluminescence of perylene, terrylene, and quaterrylene diimides in aprotic solution, Journal of the American Chemical Society 121 (1999) 3513–3520.
[20] S.V. Bhosale, C.H. Jani, S.J. Langford, Chemistry of naphthalene diimides, Chemical Society Reviews 37 (2008) 331–342.
[21] A. Viehbeck, M.J. Goldberg, C.A. Kovac, Electrochemical properties of polyimides and related imide compounds, Journal of the Electrochemical Society 137 (1990) 1460–1466.
[22] C.E. Sroog, Polyimides, Journal of Polymer Science: Macromolecular Reviews 11 (1976) 161–208.
[23] A.K. Jeewandara, K.M.N. de Silva, Are donor–acceptor self organised aromatic systems NLO (non-linear optical) active? Journal of Molecular Structure: Theochem 686 (2004) 131–136.
[24] C. Sporer, I. Ratera, D. Ruiz-Molina, Y. Zhao, J. Vidal-Gancedo, K. Wurst, P. Jaitner, K. Clays, A. Persoons, C. Rovira, J. Veciana, A molecular multiproperty switching array based on the redox behavior of a ferrocenyl polychlorotriphenylmethyl radical, Angewandte Chemie International Edition 43 (2004) 5266–5268.
[25] M. Malaun, Z.R. Reeves, R.L. Paul, J.C. Jeffery, J.A. McCleverty, M.D. Ward, I. Asselberghs, K. Clays, A. Persoons, Reversible switching of the first hyperpolarisability of an NLO-active donor–acceptor molecule based on redox interconversion of the octamethylferrocene donor unit, Chemical Communications 1 (2001) 49–50.
[26] K.A. Green, M.P. Cifuentes, M. Samoc, M.G. Humphrey, Metal alkynyl complexes as switchable NLO systems, Coordination Chemistry Reviews 255 (2011) 2530–2541.
[27] N.N. Ma, C.G. Liu, Y.Q. Qiu, S.L. Sun, Z.M. Su, Theoretical investigation on redox-switchable second-order nonlinear optical responses of push–pull $Cp^*CoEt_2C_2B_4H_3$-expanded (metallo)porphyrins, Journal of Computational Chemistry 33 (2012) 211–219.
[28] S. Muhammad, H.L. Xu, M.R.S.A. Janjua, Z.M. Su, M. Nadeem, Quantum chemical study of benzimidazole derivatives to tune the second-order nonlinear optical molecular switching by proton abstraction, Physical Chemistry Chemical Physics 12 (2010) 4791–4799.
[29] I. Asselberghs, K. Clays, A. Persoons, M.D. Ward, J. McCleverty, Switching of molecular second-order polarisability in solution, Journal of Materials Chemistry 14 (2004) 2831–2839.
[30] E. Hendrickx, K. Clays, A. Persoons, C. Dehu, J.L. Brédas, The bacteriorhodopsin chromophore retinal and derivatives: an experimental and theoretical investigation of the second-order optical properties, Journal of the American Chemical Society 117 (1995) 3547–3555.
[31] D. Gosztola, M.P. Niemczyk, W. Svec, A.S. Lukas, M.R. Wasielewski, Excited doublet states of electrochemically generated aromatic imide and diimide radical anions, Journal of Physical Chemistry A 104 (2000) 6545–6551.
[32] C.G. Liu, X.H. Guan, Redox and photoisomerization switching of the second-order optical nonlinearity of a tetrathiafulvalene derivative of spiropyran across five states: a DFT study, Physical Chemistry Chemical Physics 14 (2012) 5297–5306.

[33] X.J. Li, S.L. Sun, N.N. Ma, X.X. Sun, G.C. Yang, Y.Q. Qiu, Theoretical investigations on electronic spectra and the redox-switchable second-order nonlinear optical responses of rhodium(I)-9,10-phenanthrenediimine complexes, Journal of Molecular Graphics and Modelling 33 (2012) 19–25.
[34] A.D. Becke, Density-functional exchange-energy approximation with correct asymptotic-behavior, Physical Review A 38 (1988) 3098–3100.
[35] C. Lee, W. Yang, R.G. Parr, Development of the colle-salvetti correlation-energy formula into a functional of the electron density, Physical Review B 37 (1988) 785–789.
[36] B. Miehlich, A. Savin, H. Stoll, H. Preuss, Results obtained with the correlation-energy density functionals of Becke and Lee Yang and Parr, Chemical Physics Letters 157 (1989) 200–206.
[37] A.D. Becke, Density-functional thermochemistry. III. The role of exact exchange, Journal of Chemical Physics 98 (1993) 5648–5652.
[38] G.A. Petersson, A. Bennett, T.G. Tensfeldt, M.A. Al-Laham, W.A. Shirley, J. Mantzaris, A complete basis set model chemistry. I. The total energies of closed-shell atoms and hydrides of the first-row atoms, Journal of Chemical Physics 89 (1988) 2193–2218.
[39] G.A. Petersson, M.A. Al-Laham, A complete basis set model chemistry. II. Open-shell systems and the total energies of the first-row atoms, Journal of Chemical Physics 94 (1991) 6081–6090.
[40] T. Clark, J. Chandrasekhar, G.W. Spitznagel, P.v.R. Schleyer, Efficient diffuse function-augmented basis-sets for anion calculations. 3. The 3-21+G basis set for 1st-row elements Li-F, Journal of Computational Chemistry 4 (1983) 294–301.
[41] M.A.L. Marques, A. Rubio, Time-dependent density-functional theory, Physical Chemistry Chemical Physics 11 (2009), 4436–4436.
[42] R.E. Stratmann, G.E. Scuseria, M.J. Frisch, An efficient implementation of time-dependent density-functional theory for the calculation of excitation energies of large molecules, Journal of Chemical Physics 109 (1998) 8218–8224.
[43] S. Guha, F.S. Goodson, S. Roy, L.J. Corson, C.A. Gravenmier, S. Saha, Electronically regulated thermally and light-gated electron transfer from anions to naphthalenediimides, Journal of the American Chemical Society 133 (2011) 15256–15259.
[44] B. Champagne, M. Guillaume, F. Zutterman, TDDFT investigation of the optical properties of cyanine dyes, Chemical Physics Letters 425 (2006) 105–109.
[45] S. Hirata, M. Head-Gordon, Time-dependent density functional theory for radicals: an improved description of excited states with substantial double excitation character, Chemical Physics Letters 302 (1999) 375–382.
[46] Y. Zhao, D.G. Truhlar, Density functional for spectroscopy: no long-range self-interaction error, good performance for rydberg and charge-transfer states, and better performance on average than B3LYP for ground states, Journal of Physical Chemistry A 110 (2006) 13126–13130.
[47] M. Cossi, V. Barone, Solvent effect on vertical electronic transitions by the polarizable continuum model, Journal of Chemical Physics 112 (2000) 2427–2435.
[48] Y.Q. Qiu, C.S. Qin, Z.M. Su, G.C. Yang, X.M. Pan, R.S. Wang, DFT/FF study on electronic structure and second-order NLO property of dinuclear gold complex $[Au(SeC_2B_{10}H_{11})(PPh_3)]_2$, Synthetic Metals 152 (2005) 273–276.
[49] A.D. McLean, M. Yoshimine, Theory of molecular polarizabilities, Journal of Chemical Physics 47 (1967) 1927–1935.
[50] A.D. Becke, A new mixing of Hartree-Fock and local density-functional theories, Journal of Chemical Physics 98 (1993) 1372–1377.
[51] Y. Zhao, D.G. Truhlar, The M06 suite of density functionals for main group thermochemistry, thermochemical kinetics, noncovalent interactions, excited states, and transition elements: two new functionals and systematic testing of four M06-class functionals and 12 other functionals, Theoretical Chemistry Accounts 120 (2008) 215–241.
[52] T. Yanai, D.P. Tew, N.C. Handy, A new hybrid exchange–correlation functional using the Coulomb-attenuating method (CAM-B3LYP), Chemical Physics Letters 393 (2004) 51–57.
[53] H.D. Cohen, C.C.J. Roothaan, Electric dipole polarizability of atoms by the Hartree-Fock method. I. Theory for closed-shell systems, Journal of Chemical Physics 43 (1965) S34–S39.
[54] A. Willetts, J.E. Rice, D.M. Burland, D.P. Shelton, Problems in the comparison of theoretical and experimental hyperpolarizabilities, Journal of Chemical Physics 97 (1992) 7590–7599.
[55] M.J. Frisch, G.W. Trucks, H.B. Schlegel, G.E. Scuseria, M.A. Robb, J.R. Cheeseman, G. Scalmani, V. Barone, B. Mennucci, G.A. Petersson, H. Nakatsuji, M. Caricato, X. Li, H.P. Hratchian, A.F. Izmaylov, J. Bloino, G. Zheng, J.L. Sonnenberg, M. Hada, M. Ehara, K. Toyota, R. Fukuda, J. Hasegawa, M. Ishida, T. Nakajima, Y. Honda, O. Kitao, H. Nakai, T. Vreven, J.A. Montgomery Jr., J.E. Peralta, F. Ogliaro, M. Bearpark, J.J. Heyd, E. Brothers, K.N. Kudin, V.N. Staroverov, R. Kobayashi, J. Normand, K. Raghavachari, A. Rendell, J.C. Burant, S.S. Iyengar, J. Tomasi, M. Cossi, N. Rega, J.M. Millam, M. Klene, J.E. Knox, J.B. Cross, V. Bakken, C. Adamo, J. Jaramillo, R. Gomperts, R.E. Stratmann, O. Yazyev, A.J. Austin, R. Cammi, C. Pomelli, J.W. Ochterski, R.L. Martin, K. Morokuma, V.G. Zakrzewski, G.A. Voth, P. Salvador, J.J. Dannenberg, S. Dapprich, A.D. Daniels, O. Farkas, J.B. Foresman, J.V. Ortiz, J. Cioslowski, D.J. Fox, Gaussian 09, Revision A. 02, Gaussian, Inc., Wallingford, CT, 2009.
[56] S.I. Gorelsky, AOMix: Program for molecular orbital analysis, http://www.sg-chem.net/, University of Ottawa, Version 6.5, 2011.
[57] M. Grucela-Zajac, M. Filapek, L. Skorka, J. Gasiorowski, E.D. Glowacki, H. Neugebauerc, E. Schab-Balcerzak, Thermal, optical, electrochemical, and electrochromic characteristics of novel polyimides bearing the Acridine Yellow moiety, Materials Chemistry and Physics 137 (2012) 221–234.
[58] C.W. Dirk, L.T. Cheng, M.G. Kuzyk, A simplified three-level model describing the molecular third-order nonlinear optical susceptibility, International Journal of Quantum Chemistry 43 (1992) 27–36.
[59] E. Shirman, A. Ustinov, N. Ben-Shitrit, H. Weissman, M.A. Iron, R. Cohen, B. Rybtchinski, Stable aromatic dianion in water, Journal of Physical Chemistry B 112 (2008) 8855–8858.
[60] R.O. Marcon, S. Brochsztain, Aggregation of 3,4,9,10-perylenediimide radical anions and dianions generated by reduction with dithionite in aqueous solutions, Journal of Physical Chemistry A 113 (2009) 1747–1752.
[61] M. Nakano, N. Nakagawa, R. Kishi, S. Ohta, M. Nate, H. Takahashi, T. Kubo, K. Kamada, K. Ohta, B. Champagne, E. Botek, Y. Morita, K. Nakasuji, K. Yamaguchi, Second Hyperpolarizabilities of singlet polycyclic diphenalenyl radicals: effects of the nature of the central heterocyclic ring and substitution to diphenalenyl rings, Journal of Physical Chemistry A 111 (2007) 9102–9110.
[62] S. Ohta, M. Nakano, T. Kubo, K. Kamada, K. Ohta, R. Kishi, N. Nakagawa, B. Champagne, E. Botek, A. Takebe, S. Umezaki, M. Nate, H. Takahashi, S. Furukawa, Y. Morita, K. Nakasuji, K. Yamaguchi, Theoretical study on the second hyperpolarizabilities of phenalenyl radical systems involving acetylene and vinylene linkers: diradical character and spin multiplicity dependences, Journal of Physical Chemistry A 111 (2007) 3633–3641.
[63] M. Nakano, R. Kishi, T. Nitta, T. Kubo, K. Nakasuji, K. Kamada, K. Ohta, B. Champagne, E. Botek, K. Yamaguchi, Second hyperpolarizability (γ) of singlet diradical system: dependence of γ on the diradical character, Journal of Physical Chemistry A 109 (2005) 885–891.
[64] M. Ottonelli, M. Piccardo, D. Duce, S. Thea, G. Dellepiane, Tuning the photophysical properties of pyrene-based systems: a theoretical study, Journal of Physical Chemistry A 116 (2011) 611–630.